JOURNAL OF THERMOPHYSICS AND HEAT TRANSFER
Vol. 20, No. 3, July–September 2006

Fuel Cell Exergy Losses of Activation Energy and Cathode Polarization

G. F. Naterer*
University of Ontario Institute of Technology, Oshawa, Ontario L1H 7K4, Canada
and
C. D. Tokarz†
University of Manitoba, Winnipeg, Manitoba R3T 2N2, Canada

This article investigates thermochemical irreversibilities of activation energy and concentration polarization in fuel cells. The predictive formulation uses the Butler–Volmer equation for the activation overpotential and it includes both Knudsen and self-diffusion for the concentration polarization. Entropy production of activation energy occurs due to a portion of cell voltage lost in driving the chemical reaction to transfer electrons to/from the electrode. In this article, exergy losses associated with these activation and concentration irreversibilities are formulated based on the Second Law. Unlike past studies of entropy production in solid oxide fuel cells, this article extends past methods to half-cell reactions and thermochemical irreversiblities in a proton-exchange membrane fuel cell. Voltage losses are derived based on entropy production within the fuel cell, in contrast to past methods involving polarization curves. The entropy-based method provides a useful alternative to past conventional methods, because it can encompass both electrochemical irreversibilities (such as electrode polarization) and thermofluid irreversibilities (such as fuel channel friction).

Nomenclature

C	=	concentration, mol/m^3
D	=	diffusion coefficient, m^2/s
E	=	voltage, V
E^0	=	standard equilibrium potential, V
F	=	Faraday's constant, 96,785 C/mol
G	=	Gibbs free energy, J
i	=	current density, A/m^2
J	=	flux, mol/s
K	=	equilibrium constant
l	=	thickness, m
M	=	molar mass
$\dot{m}$	=	mass flow rate, kg/s
N	=	number of moles per mole H_2
n_d	=	electro-osmotic drag coefficient
n_e	=	moles of electrons per half-cell reaction
P	=	pressure, Pa
$\dot{P}_s$	=	entropy production rate, W/mol K
$\dot{Q}$	=	heat transfer rate, W
R	=	universal gas constant, 8.314 J/mol K
s	=	molar entropy, J/mol K
T	=	temperature, K
v	=	specific volume, m^3/kg
$\dot{W}$	=	power, W
X_{dest}	=	exergy destruction rate, W/mol
β	=	transfer coefficient
γ	=	stoichiometric ratio
η	=	polarization, V
ρ	=	density, kg/m^3

Subscripts

a, c	=	anode, cathode
eff	=	effective
fc	=	fuel cell
H_2	=	hydrogen
H_2O	=	water vapor
m	=	membrane/electrolyte
O_2	=	oxygen
P, R	=	products, reactants
0	=	exchange

Superscripts

I	=	inlet conditions
rev	=	reversible

Received 26 July 2005; revision received 24 September 2005; accepted for publication 28 September 2005.

*Professor and Director of Research, Graduate Studies and Development, Faculty of Engineering and Applied Science, 2000 Simcoe Street N. Associate Fellow AIAA.

†Research Assistant, Department of Mechanical and Manufacturing Engineering, 15 Gillson Street.

I. Introduction

FUEL cells are promising alternatives to batteries in aerospace applications, such as space science probes, planetary rovers, and other payloads.[1] They provide a high power-density source of energy. Effective tradeoffs between efficiency and total mass are significant factors when fuel cells are evaluated as a method of energy storage in aerospace applications. Barbir et al.[2] have shown that high fuel cell efficiency does not necessarily give the highest specific energy. This article examines entropy production in fuel cells in efforts to reduce voltage losses and provide a systematic framework for improving fuel cell efficiency.

A regenerative fuel cell was developed by Chang and co-workers[3] at the NASA Glenn Research Center. It includes integration of a fuel cell and electrolyzer into an energy storage system. The regenerative system is capable of autonomous cyclic operation, while providing both dc load and dc power from solar heat input. Sridhar and Foerstner[4] have developed a regenerative solid oxide fuel cell for applications to Mars exploration. Continuous operation of the fuel cell stack during both day and night eliminated any time needed for thermal ramp-up. Large stack sizes were not needed for excess oxygen during nightly operation, due to larger oxygen production time. The regenerative system provided heat input to other spacecraft components during a cold Martian night.

In cold night conditions of Mars exploration, better fuel cell performance is needed at temperatures below freezing. Effects of

subzero temperatures (between 0 and −27.5°C) on start-up behavior of planar free-breathing proton exchange membrane (PEM) fuel cells were investigated experimentally by Hottinen and co-workers.[5] It was observed that stable operation could be achieved, provided current densities were high enough to prevent water from freezing inside the fuel cell.

However, ice formation on the outer side of the cathode was observed. Predictions of ice formation involve a nonlinear heat balance at the moving interface (Xu and Naterer[6]). At lower current densities within a fuel cell, Hottinen et al.[5] reported that freezing of water inside the fuel cell produced significant performance losses. At temperatures below about −10°C, the start-up procedure becomes noticeably slower. Sundaresan and Moore[7] have applied a lumped model to evaluate various heating methods to overcome freezing problems in fuel cells. In this article, voltage losses are characterized by entropy production, which can include the latent entropy of fusion to accommodate phase change irreversibility due to freezing.[8,9]

PEM fuel cells provide a viable alternative way to supply electrical power for NASA's Next Generation Launch Technology program.[10] Optimization of operating conditions to maximize power output of fuel cells was investigated by Mawardi et al.[11] The methodology considered one-dimensional nonisothermal operation of a fuel cell. A simulated annealing algorithm with a continuous search procedure was developed to find various optimal solutions. Similar optimization procedures have been applied to other applications, such as aircraft engine bay cooling (Wang et al.[12]). Analytical methods of optimization have minimized entropy production in convective heat transfer problems, involving slip-flow conditions within embedded microchannels taking advantage of adaptive surface micropatterns.[13]

Effects of ohmic, concentration, and activation irreversibilities on fuel cell performance were reported by Chan and Xia.[14] The authors[14] calculated entropy production in terms of the lost work potential of the fuel cell. Their formulation used the Butler–Volmer model of activation polarization. Unlike these past solid oxide (SO) fuel cell studies, this article considers entropy production in PEM fuel cells. Different half-cell reactions and operating conditions are encountered in PEM fuel cells.

An entropy/exergy analysis of an integrated PEM fuel cell was reported by Song et al.[15] The system consisted of a fuel cell, CO shift reactor, vaporizer, mixer, steam reformer, and burner. Different power and voltage levels were considered. The exergy analysis identified key locations of deficiencies within the overall system. Unlike external subsystems investigated by Song et al.,[15] this article focuses on internal irreversibilities arising from activation energy and concentration polarization losses within the electrodes.

Ghadamian and Saboohi[16] have developed correlations for predicting voltage losses in fuel cells. Ideal theoretical cases were represented in terms of the reversible open-circuit voltage. Deviations from ideal operation were studied to improve fuel cell efficiency. Voltage losses of activation, fuel crossover, concentration, and ohmic losses were considered by the authors.[16] Accumulated voltage losses were subtracted from the open circuit voltage to predict the operating voltage. It was reported that activation irreversibilities have a considerable impact on the total voltage loss. Unlike past studies calculating activation losses directly from polarization curves, this article uses entropy production to characterize the voltage losses.

In this article, numerical predictions of entropy production in a fuel cell will be used to identify regions of highest voltage losses. Hussain et al.[17] have predicted irreversibilities within individual components of a PEM fuel cell. Effects of varying operating conditions (temperature, pressure, and air stoichiometry) on fuel cell efficiencies were reported. The air compressor, cooling loop, and heat exchanger were considered. The largest irreversibilities were calculated in the fuel cell stack. In contrast to external subsystem irreversibilities considered by Hussain et al.,[17] this article focuses on entropy production of activation energy and electrode polarization within the fuel cell stack. It aims to develop an alternative entropy-based method of systematically improving performance of fuel cells.

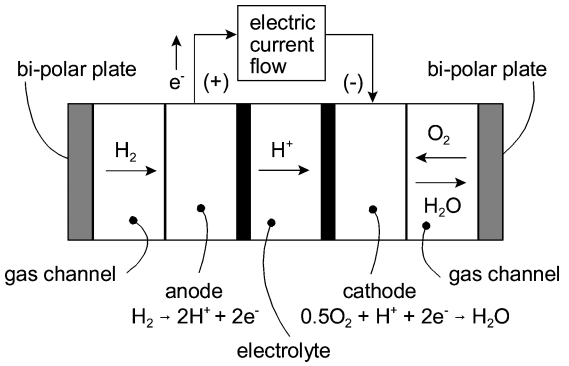

Fig. 1 Operating components of a proton-exchange membrane fuel cell.

II. Fuel Cell Operation

Two common types of fuel cells are the PEM fuel cell and the solid oxide (SO) fuel cell. In PEM fuel cells, hydrogen is combined with oxygen to produce water, which is a reversal of the electrolysis of liquid water. A typical maximum voltage for PEM fuel cells is between 0.95 and 1.1 V. Due to ohmic resistance and other losses, a common operating voltage is about 0.7 V. It typically varies between 0.6 and 0.8 V, depending on the electric current drawn from internal reactions.[18] The operating principles of an SO fuel cell are similar to those of a PEM fuel cell, except for differences in half-cell chemical reactions. PEM half-cell reactions produce positive ions that migrate across the electrolyte from the anode to the cathode (see Fig. 1). However, SO half-cell chemical reactions produce negative ions, which migrate across the electrolyte in an opposite direction (from the cathode to the anode).

In an SO fuel cell, oxidant and fuel are continuously supplied to the anode and cathode, respectively. The oxygen molecules diffuse through the cathode to the catalyst layer, between the cathode and electrolyte. At the catalyst layer, the oxygen molecules combine with free electrons from the external circuit to produce a negative oxygen ion (O^-). The oxygen ions migrate through the electrolyte to the catalyst layer between the anode and the electrolyte. Simultaneously, hydrogen molecules diffuse through the anode to the same catalyst layer, where they combine with the oxygen ions and liberate electrons, while producing H_2O and heat. Free electrons flow through the external circuit as an electrical current. Then, they return to the fuel cell at the cathode, where they combine with oxygen molecules to again produce oxygen ions and continue the cycle of power generation. Similar processes occur in the PEM fuel cell, except that hydrogen ions flow to the cathode, where water molecules are produced.

III. Exergy Destruction in a Fuel Cell

Fuel cell exergy represents the maximum work potential of a fuel cell. Unlike other variables characterizing voltage losses within a fuel cell, transport behavior of exergy and entropy are known well by standard transport equations. For example, entropy is convected with the incoming fuel stream, transported with heat flow, and produced by activation, concentration, and other irreversibilities. Thus, local sources of voltage losses can be targeted by regions of high entropy production (or entropy production multiplied by temperature, called exergy destruction). In contrast, other variables for describing fuel cell irreversibilities (such as overpotential or polarization) are not governed directly by the Second Law. For example, overpotential is a voltage superimposed over the reversible or ideal voltage. "Loss" is another term widely used to describe fuel cell performance, but it can be a vague term. This section investigates fuel cell voltages based on exergy losses, rather than other variables commonly adopted in past studies (including overpotential, polarization, or overvoltage).

Consider a control volume consisting of the anode, electrolyte, and cathode of a PEM fuel cell (see Fig. 2). For steady-state

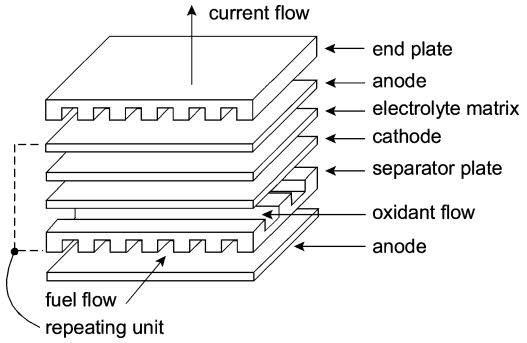

Fig. 2 Schematic of a proton-exchange membrane fuel cell.

operation, the chemical reaction within the fuel cell is

$$H_2 + \tfrac{1}{2}O_2 \Rightarrow H_2O \tag{1}$$

Pure hydrogen and pure oxygen will be considered as the fuel and oxidant streams supplied to the anode and cathode, respectively. The energy balance for the control volume can be written as

$$\dot{Q} - \dot{W} = -\sum_R \dot{m}_{Ri} \cdot N_{Ri} \cdot h_{Ri} + \sum_P \dot{m}_{Pi} \cdot N_{Pi} \cdot h_{Pi} \tag{2}$$

where h is the molar enthalpy and the subscripts R, P, and i refer to reactants, products, and component number, respectively. Substituting the appropriate number of moles based on the chemical reactions within the fuel cell (per mol of H_2),

$$\dot{Q} - \dot{W} = -\dot{m} \cdot \left[(1) \cdot h_{H_2} + 0.5 \cdot h_{O_2}\right] + \dot{m} \cdot (1) \cdot h_{H_2O} \tag{3}$$

The entropy balance for the same control volume can be expressed as

$$\dot{Q} = T \cdot \left[\sum_P \dot{m}_{Pi} \cdot N_{Pi} \cdot (s_{Pi}) - \sum_R \dot{m}_{Ri} \cdot N_{Ri} \cdot (s_{Pi})\right] - T\dot{P}_{s,\mathrm{fc}} \tag{4}$$

where $\dot{Q}$ is the waste heat output from the fuel cell. Also, $\dot{P}_{s,\mathrm{fc}}$ is the fuel cell entropy production rate. The Second Law requires that entropy production be nonnegative. Substituting the appropriate molar fluxes (per mol of H_2),

$$\dot{Q} = T \cdot \dot{m} \cdot \left[s_{H_2O} - s_{H_2} - 0.5 s_{O_2}\right] - T\dot{P}_{s,\mathrm{fc}} \tag{5}$$

where s is the specific (molar) entropy of the system and T is the surrounding temperature.

For ideal gases, $h = h(T)$ and $s = s(T, p)$. Then, combining the energy and entropy balances for the control volume yields the following power output from the fuel cell,

$$\dot{W} = \dot{m} \cdot \left[h_{H_2}(T) + 0.5 h_{O_2}(T) - h_{H_2O}(T)\right] - T \cdot \dot{m}\left[s_{H_2}(T, p_{H_2}) + 0.5 s_{O_2}(T, p_{O_2}) - s_{H_2O}(T, p_{H_2O})\right] - T \cdot \dot{P}_{s,\mathrm{fc}} \tag{6}$$

In order to express these results in terms of the Gibbs free energy and equilibrium constant, the entropy terms are subdivided into standard pressure and system pressure (p_0) terms,

$$\begin{aligned}\dot{W} = {} & \dot{m}\left[h_{H_2}(T) + 0.5 h_{O_2}(T) - h_{H_2O}(T)\right] - T \cdot \dot{m} \cdot \left[s_{H_2}(T, p_0) + 0.5 s_{O_2}(T, p_0) - s_{H_2O}(T, p_0)\right] - T \cdot \dot{P}_{s,\mathrm{fc}} \\ & - T \cdot \dot{m}\left[-s_{H_2}(T, p_0) + s_{H_2}(T, p_{H_2})\right] \\ & - T \cdot \dot{m}\left[-s_{O_2}(T, p_0) + s_{O_2}(T, p_{O_2})\right] \\ & - T \cdot \dot{m}\left[+s_{H_2O}(T, p_0) - s_{H_2O}(T, p_{H_2O})\right]\end{aligned} \tag{7}$$

From the Gibbs equation and definition of specific heat, the entropy change, ds, can be expressed in terms of the pressure change, dp, and temperature change, dT, as follows,

$$ds = c_p(dT/T) - (v/T)dp \tag{8}$$

which can be integrated between two state points (1 and 2) to give

$$s_2 - s_1 = c_p \ln(T_2/T_1) - R \ln(P_2/P_1) \tag{9}$$

Also, the Gibbs free energy can be expressed as follows:

$$\Delta G_T^0 = h_T^0 - T \cdot s_T^0 \tag{10}$$

where the superscript 0 designates that products and reactants enter/leave the control volume at the standard pressure, p_0.

Combining Eqs. (7), (9), and (10) yields the following rate of power output:

$$\dot{W} = \dot{m} \cdot \left(-\Delta G_T^0\right) - T \cdot \dot{m}\left[-R \ln\left(p'_{H_2}/p_0\right) - 0.5R \ln\left(p'_{O_2}/p_0\right) + R \ln\left(p'_{H_2O}/p_0\right)\right] - T \cdot \dot{P}_{s,\mathrm{fc}} \tag{11}$$

Thus, the power output of the fuel cell depends on the Gibbs free energy, reactant/product partial pressures, temperature, and mass flow rate of fuel and oxidant streams. Rearranging Eq. (11),

$$\dot{W} = \dot{m} \cdot \left(-\Delta G_T^0\right) - \dot{m}RT \ln\left[\left(p_0/p'_{H_2}\right) \cdot \left(p_0/p'_{O_2}\right)^{\frac{1}{2}} \cdot \left(p'_{H_2O}/p_0\right)\right] - T \cdot \dot{P}_{s,\mathrm{fc}} \tag{12}$$

Alternatively, in terms of the entropy production rate,

$$\dot{P}_{s,\mathrm{fc}} = -\dot{W}/T + (\dot{m}/T)\left(-\Delta G_T^0\right) - \dot{m}R \ln\left[\left(p'_{H_2O}/p'_{H_2}\right) \cdot \left(p_0/p'_{O_2}\right)^{\frac{1}{2}}\right] \tag{13}$$

The Gibbs free energy can be expressed in terms of the equilibrium constant, K, as follows:

$$-\Delta G_T^0 = RT \ln K(T) \tag{14}$$

Substituting this expression into Eq. (13) and dividing by the mass flow rate,

$$P_{s,\mathrm{fc}} = -W/T + R \ln K - R \ln\left[\left(p'_{H_2O}/p'_{H_2}\right) \cdot \left(p'_0/p'_{O_2}\right)^{\frac{1}{2}}\right] \tag{15}$$

The fuel cell does not perform mechanical work, so the work term (W) must be electrical work output from the fuel cell. This electrical work can be written as

$$W_{\mathrm{el}} = zFE \tag{16}$$

where z is the number of coulombs. Using this expression for work output in Eq. (12) with $z = 2$ and rearranging,

$$E = (RT/2F) \ln K - (RT/2F) \times \ln\left[\left(p'_{H_2O}/p'_{H_2}\right) \cdot \left(p_0/p'_{O_2}\right)^{\frac{1}{2}}\right] - (T \cdot P_{s,\mathrm{fc}})/2F \tag{17}$$

Thus, the cell voltage depends on entropy production. The last term is subtracted from the cell voltage, thereby indicating that thermodynamic irreversibilities contribute to voltage losses within the fuel cell. Optimal fuel cell performance can be established after minimizing the entropy production rate in Eq. (17). The first and second terms on the right side describe the effects of temperature and product/reactant pressures, respectively, on the cell voltage change.

The entropy production term on the right side of Eq. (17) is usually written in terms of activation (subscript act), ohmic (subscript ohm), and concentration polarizations (subscript conc). Activation losses occur when a portion of cell voltage is lost in driving the chemical reaction, whereas ohmic losses arise from resistive heating within

the electrodes/electrolyte. Comparing Eq. (17) with cell voltages derived by Chan and Xia,[14]

$$(T \cdot P_{s,\mathrm{fc}})/2F = \eta_{\mathrm{act}} + \eta_{\mathrm{ohm}} + \eta_{\mathrm{conc}} = \eta \tag{18}$$

or

$$P_{s,\mathrm{fc}} = 2F/T \cdot \eta \tag{19}$$

Thus, the power lost from polarization irreversibilities can be determined from the entropy production multiplied by temperature (or exergy destruction). Performing this multiplication and comparing with Eq. (16), the lost work can be expressed as

$$W_{\mathrm{lost}} = 2F\eta \tag{20}$$

The next section focuses on the activation component of total polarization in Eq. (18).

IV. Formulation of Activation Exergy Destruction

Activation polarization (or charge polarization) arises due to the activation energy, when the reactants must overcome a certain energy barrier before the chemical reaction can occur. This type of polarization represents an extra potential required to overcome the step energy barrier so that the desired rate of electrode reaction is achieved. The process occurs from charge transfer from electric to ionic conductors, which can be described by the Butler–Volmer equation,

$$i = i_0 \left\{ \exp\left(\beta \frac{n_e F \eta_{\mathrm{act}}}{RT}\right) - \exp\left(-(1-\beta)\frac{n_e F \eta_{\mathrm{act}}}{RT}\right)\right\} \tag{21}$$

where i_0 is the exchange current density and n_e refers to the number of electrons transferred per reaction. The transfer coefficient, β, represents the fractional change of polarization that leads to a constant change of reaction rate.

The exchange current density, i_0, represents the equilibrium potential of the forward and reverse electrode reaction rates. High values of i_0 suggest a high electrode reaction rate, thereby leading to good fuel cell performance. For a PEM fuel cell electrolyte, the exchange current density can be calculated in the following manner,[14]

$$i_0 = i_0^{\mathrm{ref}} \left(C_{\mathrm{O_2}} \big/ C_{\mathrm{O_2}}^{\mathrm{ref}}\right)^{\gamma_{\mathrm{O_2}}} \left(C_{\mathrm{H^+}} \big/ C_{\mathrm{H^+}}^{\mathrm{ref}}\right)^{\gamma_{\mathrm{H^+}}} \tag{22}$$

When the concentration of hydrogen protons is constant, Eq. (22) becomes

$$i_0 \big/ i_0^{\mathrm{ref}} = \left(C_{\mathrm{O_2}} \big/ C_{\mathrm{O_2}}^{\mathrm{ref}}\right)^{\gamma_{\mathrm{O_2}}} \tag{23}$$

where i_0^{ref} is the reference exchange current density. In a PEM fuel cell, this value is typically $i_0^{\mathrm{ref}} = 0.6$ A/cm^2 in the anode and $i_0^{\mathrm{ref}} = 4.4 \times 10^{-7}$ A/cm^2 in the cathode. In an SO fuel cell, the exchange current density is typically obtained from curve fitting of experimental data. Substituting $\beta = 0.5$ [14] into Eq. (21),

$$i = i_0 \left\{ \exp\left(0.5 \frac{n_e F \eta_{\mathrm{act}}}{RT}\right) - \exp\left(-(1-0.5)\frac{n_e F \eta_{\mathrm{act}}}{RT}\right)\right\} \tag{24}$$

which can be expressed as

$$i = 2i_0 \sinh\left(\frac{n_e F \eta_{\mathrm{act}}}{2RT}\right) \tag{25}$$

It should be noted that the transition from Eq. (24) to (25) requires that β be identically equal to 0.5. Rearranging Eq. (25) in terms of the activation overpotential, it can be shown that

$$\eta_{\mathrm{act}} = (2RT/n_e F)\, \ln\left(i/2i_0 + \sqrt{i^2}\big/4i_0^2 + 1\right) \tag{26}$$

Under limiting cases of a high activation polarization, the second term is negligible and the result can be simplified to the Tafel equation. Thus, the Butler–Volmer equation becomes

$$\eta_{\mathrm{act}} = -(RT/\beta n_e F)\, \ln i_0 + (RT/\beta n_e F)\, \ln i \tag{27}$$

This result represents a limiting case, so the previously derived general form of the activation polarization in Eq. (26) will be preferred.

The activation component of total entropy production becomes

$$P_{s,\mathrm{act}} = (4R/n_e)\, \ln\left(i/2i_0 + \sqrt{i^2}\big/4i_0^2 + 1\right) \tag{28}$$

Alternatively, the exergy destruction due to activation irreversibilities becomes

$$X_{\mathrm{dest,act}} = (4RT/n_e)\, \ln\left(i/2i_0 + \sqrt{i^2}\big/4i_0^2 + 1\right) \tag{29}$$

The next section considers entropy production due to concentration polarization.

V. Formulation of Concentration Exergy Losses

In a PEM fuel cell, countercurrent mass diffusion occurs within the cathode. Temperatures within the fuel cell will be assumed to be sufficient to yield negligible transport of liquid water through the solid electrode. The fluxes of oxygen and water vapor are given by

$$J_{\mathrm{O_2}} = -D_{\mathrm{O_2(eff)}} \nabla C_{\mathrm{O_2}} + C_{\mathrm{O_2}} v \tag{30}$$

$$J_{\mathrm{H_2O}} = -D_{\mathrm{H_2O(eff)}} \nabla C_{\mathrm{H_2O}} + C_{\mathrm{H_2O}} v \tag{31}$$

where v refers to velocity (m/s). Using stoichiometry for countercurrent mass transfer, the oxygen flux becomes

$$J_{\mathrm{O_2}} = -2J_{\mathrm{H_2O}} \tag{32}$$

Substituting this result into the previous equations and rearranging,

$$v = \left(D_{\mathrm{O_2(eff)}} + 2D_{\mathrm{H_2O(eff)}}\right)\big/C_c \cdot \nabla C_{\mathrm{O_2}} \tag{33}$$

where $C_c = C_{\mathrm{O_2}} + 2C_{\mathrm{H_2O}}$.

Substituting Eq. (33) into Eq. (30) yields the following oxygen flux,

$$J_{\mathrm{O_2}} = -2\left[D_{\mathrm{H_2O(eff)}}\left(C_{\mathrm{H_2O}}/C_c\right) + D_{\mathrm{O_2(eff)}}\left(C_{\mathrm{O_2}}/C_c\right)\right] \cdot \nabla C_{\mathrm{O_2}} \tag{34}$$

Thus, the flux of water vapor becomes

$$J_{\mathrm{H_2O}} = \left\{D_{\mathrm{H_2O(eff)}} + C_{\mathrm{H_2O}} \cdot \left[D_{\mathrm{O_2(eff)}} - 2D_{\mathrm{H_2O(eff)}}\right]\big/C_c\right\} \cdot \nabla C_{\mathrm{O_2}} \tag{35}$$

Using the chemical balance of atoms for oxygen and water vapor, it can be shown that

$$J_{\mathrm{H_2O}} = \left[D_{\mathrm{H_2O(eff)}}\left(C_{\mathrm{O_2}}/C_c\right) + D_{\mathrm{O_2(eff)}}\left(C_{\mathrm{H_2O}}/C_c\right)\right] \cdot \nabla C_{\mathrm{O_2}} \tag{36}$$

Define an effective cathode diffusion coefficient as follows,

$$D_{c(\mathrm{eff})} = \left[D_{\mathrm{H_2O(eff)}}\left(C_{\mathrm{O_2}}/C_c\right) + D_{\mathrm{O_2(eff)}}\left(C_{\mathrm{H_2O}}/C_c\right)\right] \tag{37}$$

Then the oxygen flux becomes

$$J_{\mathrm{O_2}} = -2D_{c(\mathrm{eff})} \cdot \nabla C_{\mathrm{O_2}} \tag{38}$$

Considering one-dimensional mass transfer,

$$J_{\mathrm{O_2}} = -2D_{c(\mathrm{eff})} \frac{\mathrm{d}C_{\mathrm{O_2}}}{\mathrm{d}x} \tag{39}$$

In addition, the flux of hydrogen and change of oxygen concentration are

$$J_{H_2} = (i/4F) \tag{40}$$

and

$$dC_{O_2} = dp_{O_2}/RT \tag{41}$$

Using these results, the oxygen flux becomes

$$J_{O_2} = \frac{i}{4F} = -\frac{2D_{c(\text{eff})}}{RT} \cdot \frac{dp_{O_2}}{dx} \tag{42}$$

which may be rearranged and integrated as follows;

$$\int_{p^I_{O_2}}^{p_{O_2}} dp_{O_2} = -\int_0^{l_c} \frac{iRT}{8FD_{c(\text{eff})}}\, dx \tag{43}$$

Integration yields the following pressure of oxygen at the reaction sites:

$$p_{O_2} = p^I_{O_2} - \frac{RTl_c}{8FD_{c(\text{eff})}} i \tag{44}$$

Similarly, the water vapor pressure at the reaction sites can be determined as follows:

$$p_{H_2O} = p^I_{H_2O} + \frac{RTl_c}{4FD_{c(\text{eff})}} i \tag{45}$$

The concentration polarization (η_{conc}) is the potential difference, ΔE, between the reversible voltage and the operating cell voltage, that is,

$$\eta_{\text{conc}} = \Delta E = E_{\text{rev}} - E_{\text{current}} \tag{46}$$

where

$$E_{\text{rev}} = E^0 + (RT/2F)\, \ell n\left(C^I_{O_2}\right) \tag{47}$$

$$E_{\text{current}} = E^0 + (RT/2F)\, \ell n\left(C_{O_2}\right) \tag{48}$$

Writing concentration ratios in terms of partial pressures, the concentration polarization is

$$\eta_{\text{conc}} = -\frac{RT}{n_e F}\, \ell n\left[\frac{p_{H_2}/p^I_{H_2}}{p_{H_2O}/p^I_{H_2O}}\right]$$

$$= -\frac{RT}{4F}\, \ell n\left[\left(1 - \frac{RTl_c}{8FD_{c(\text{eff})}p^I_{O_2}} i\right) \Big/ \left(1 + \frac{RTl_c}{4FD_{c(\text{eff})}p^I_{H_2O}} i\right)\right] \tag{49}$$

This result is similar to past results derived for a solid oxide fuel cell,[14] except that coefficients, partial pressures, and diffusion coefficients have been changed accordingly, due to different half-cell reactions in a PEM fuel cell. The previous concentration polarization yields the following diffusive exergy destruction:

$$X_{\text{dest,conc}} = -\frac{RT}{2}\, \ell n\left[\left(1 - \frac{RTl_c}{8FD_{c(\text{eff})}p^I_{O_2}} i\right) \Big/ \left(1 + \frac{RTl_c}{4FD_{c(\text{eff})}p^I_{H_2O}} i\right)\right] \tag{50}$$

It is expected that physically plausible operation of the PEM fuel cell requires that operating parameters within the square brackets must yield a non-negative exergy destruction rate.

In addition to activation and cathode irreversibilities (discussed previously), the total entropy production within the fuel cell includes anode and ohmic irreversibilities.[14] For a small anode thickness in a PEMFC (corresponding to a small cathode thickness for an SOFC), past data[19] have shown that voltage losses become independent of the limiting current density of the anode, i_{0a}. In this case, the anode concentration polarization diminishes when the anode thickness becomes much smaller than the cathode thickness. The following TAP/TCS model (thin anode for PEMFC/thin cathode for SOFC approximation) neglects the anode concentration polarization. Thus, combining the previous irreversibilities with the ohmic losses,

$$P_s = \frac{2RT}{n_e F}\, \ell n\left(\frac{i}{i_{0a}} + \sqrt{\frac{i^2}{i^2_{0a}} + 1}\right) + \frac{2RT}{n_e F}\, \ell n\left(\frac{i}{i_{0c}} + \sqrt{\frac{i^2}{i^2_{0c}} + 1}\right)$$

$$- \frac{2F^2 C_{H^+} D_m}{Tl_m n_d}\, \ell n\left(1 - \frac{i}{i_L}\right) - \frac{RT}{4F}\, \ell n\left[\left(1 - \frac{RTl_c}{8FD_{c,\text{eff}}p^I_{O_2}} i\right) \Big/ \left(1 + \frac{RTl_c}{8FD_{c,\text{eff}}p^I_{O_2}} i\right)\right] \tag{51}$$

On the right side, the five terms represent the activation polarization (first and second terms; anode plus cathode), ohmic polarization (third term), and concentration polarization for the cathode (fourth term), respectively. When the current density (i) increases, the first and second terms become larger, so activation irreversibilities become larger at high operating currents (as expected). Both concentration and ohmic terms decrease when the current density increases, thereby leading to higher entropy production due to the negative signs before each term.

The previous analysis was developed for a PEM fuel cell with the following anode and cathode half-cell reactions, respectively:

$$H_2(g) \Rightarrow 2H^+(aq) + 2e^- \qquad \text{(anode)} \tag{52}$$

$$\tfrac{1}{2}O_2(g) + 2H^+(aq) + 2e^- \Rightarrow H_2O(l) \qquad \text{(cathode)} \tag{53}$$

For an SO fuel cell, different anode and cathode half-cell reactions are encountered, that is,

$$H_2(g) + O^{2-} \Rightarrow H_2O(g) + 2e^- \qquad \text{(anode)} \tag{54}$$

$$\tfrac{1}{2}O_2(g) + 2e^- \Rightarrow O^{2-} \qquad \text{(cathode)} \tag{55}$$

The previous procedures were modified accordingly, so the TAP/TCS model could be applied to entropy production in SO fuel cells. In the next section, sample results for both PEM and SO fuel cells will be presented.

VI. Results and Discussion

In this section, numerical results of exergy losses in two types of fuel cells (PEM and SO) are presented. Problem parameters are summarized in Table 1 and additional data were adopted from Refs. 14, 16, and 20. Unlike past studies, this section aims to calculate entropy production and develop an entropy-based method of systematically improving performance of fuel cells. Unlike other variables characterizing voltage losses, entropy transport is directly governed by the Second Law. Entropy is convected with the incoming fuel stream, transported with heat flow, and produced by activation, concentration, and other irreversibilities. Local sources of voltage losses can be targeted by regions of high entropy production. The fundamental mechanism underlying a loss, polarization, or overpotential is a thermodynamic irreversibility characterized by entropy production. Thus, a Second Law efficiency can provide a useful measure of fuel cell performance, especially because fuel cells are not subject to the Carnot efficiency limit.

The symbolic computational tool Maple 9.5 was used to perform mathematical operations and calculations in this section. Ohmic, concentration, and activation irreversibilities increase at larger current densities in Fig. 3. Exergy losses are represented on the vertical axis. Each irreversibility represents a lost component of work potential within the fuel cell. Activation losses arise from slowness of reactions occurring on the surface of the electrodes. The activation irreversibility refers to the proportion of voltage lost at the electrode surface, when driving the chemical reaction at the electrode. At higher current densities, larger chemical activity occurs at the

Table 1 Operating conditions and problem parameters

Proton-exchange membrane fuel cell	
Operating temperature T, K	373
Operating pressure p, atm	1.0
Limiting current i_L, mA	800
Exchange current density i_0, A/cm^2	0.07
Specific surface resistance R, Ωcm^2	0.00003
Transfer coefficient, β	0.5
Equilibrium potential E^0, V	1.167
Solid oxide fuel cell	
Operating temperature T, °C	800
Operating pressure p, atm	2.0
Electrolyte resistance R_i, Ωcm^2	0.068
Concentration resistance R_{conc}, Ωcm^2	0.273
$RT/4F$	0.0232
Transfer coefficient, β	0.5
Exchange current density i_0, A/cm^2	0.132
Effective diffusion coefficient $D_{a,\text{eff}}$, cm^2/s	0.199
Cathode thickness l_c m	0.00005
Electrolyte thickness l_e, μm	40.0
Anode thickness l_a, μm	750.0
Partial pressure ratio, p_{H_2}/p_{H_2O}	32.242

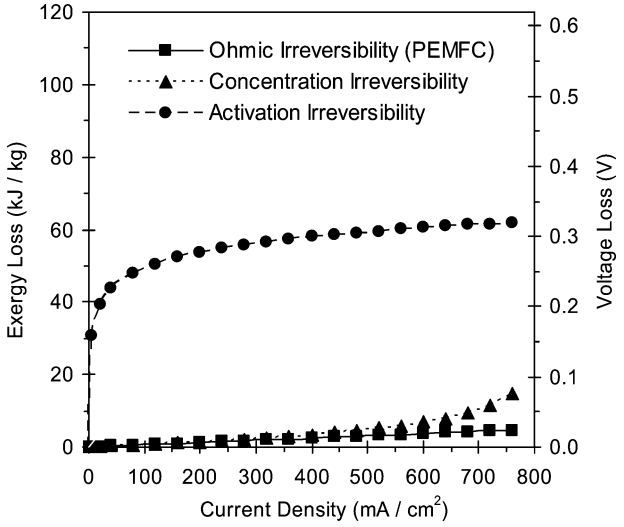

Fig. 3 Components of PEMFC exergy destruction ($T = 373$ K).

electrode surface and the irreversibility rises. In Fig. 3, it can be observed that activation irreversibilities are largest. These results were obtained for a PEM fuel cell at 373 K, whereas additional results indicate that the activation irreversibility becomes less significant at higher temperatures. Activation irreversibilities can be reduced with larger reactant concentrations, as catalyst sites become more effectively occupied by reactants.

The unit irreversibility ratio represents the total entropy production within the electrodes per unit current flow through the fuel cell (units of entropy production divided by a reference current density). The purpose of this new parameter is gaining insight into the rate of irreversibility change at rising current densities. Figure 4 depicts the unit irreversibility ratio at varying current exchange densities of 0.07, 0.21, and 0.35 A/cm^2. The exchange current density is an important parameter affecting fuel cell performance. Figure 4 indicates that the rate of change increases at smaller values of $i(0)$. The electrode surface activity increases more rapidly with larger changes in chemical reaction rates to drive higher electric currents. Figure 4 shows that the unit irreversibility ratio increases at larger current densities, due to larger chemical reaction activity and ohmic heating.

Ghadamian and Saboohi[16] have predicted voltage losses in a PEM fuel cell, including distinct zones of cell voltage losses. Similarly to previous results in Fig. 3, the authors[16] reported that losses were mainly affected by the activation polarization. At higher temperatures, ohmic polarization became a larger component of voltage

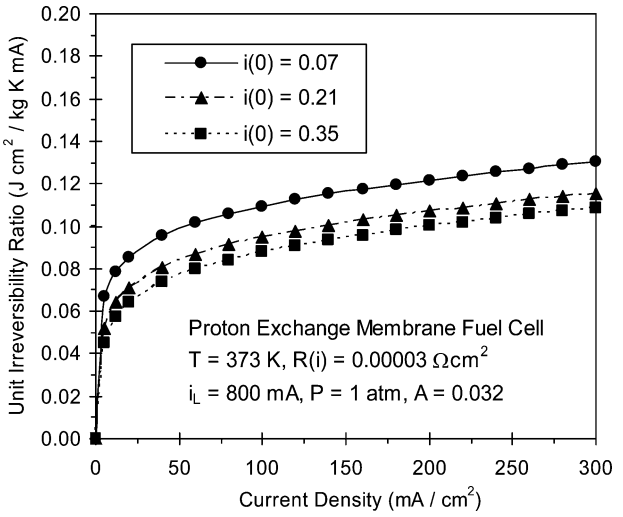

Fig. 4 PEMFC exergy destruction per unit current flow.

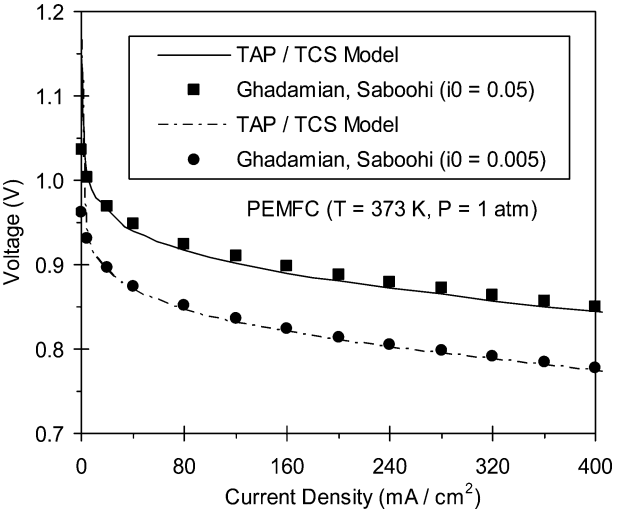

Fig. 5 Voltage profile (PEMFC; $T = 373$ K).

losses. The authors[16] observed a certain zone at high current densities approaching the limiting current, where voltage losses were dominated by the concentration polarization. When the current density increased, different mechanisms of polarization became critical, ranging from activation to ohmic and finally concentration polarization. Similarly to Fig. 3, the authors[16] confirmed that past data has shown that voltage losses increased at higher current densities.

Figure 5 shows close agreement between past data and the TAP/TCS model for $T = 373$ K, $P = 1$ atm and varying current exchange densities. The predicted voltage was determined based on the entropy production, temperature, Faraday's constant, and Eq. (56). As expected, the voltage decreases at larger current densities, due to increased chemical activity on the electrode surfaces and ohmic heating. The results suggest that similar trends are obtained, whether evaluated by standard methods or the entropy-based method. Entropy-based design provides a useful alternative, because it allows a more robust and systematic procedure for improving fuel cell performance. Certain voltage losses cannot be found readily or directly by standard methods (such as power consumed to drive oxidant through the fuel channels to overcome friction), whereas entropy and the Second Law encompass all thermodynamic irreversibilities.

The previous results were obtained for PEM fuel cells, whereas the remaining figures (Figs. 6–10) illustrate exergy loss, irreversibility, and voltage results for solid oxide fuel cells. Unlike PEM fuel cells, ohmic irreversibilities have larger significance at low operating current densities. The ohmic irreversibility rises linearly, which is expected because the ohmic voltage loss is linearly proportional to

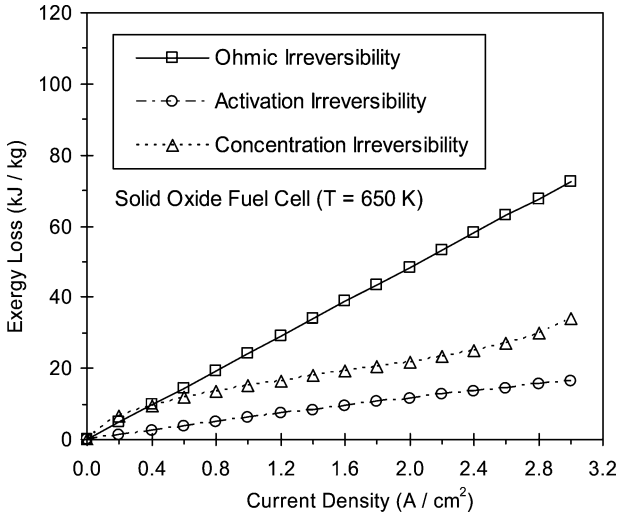

Fig. 6 SOFC exergy destruction ($T = 650$ K).

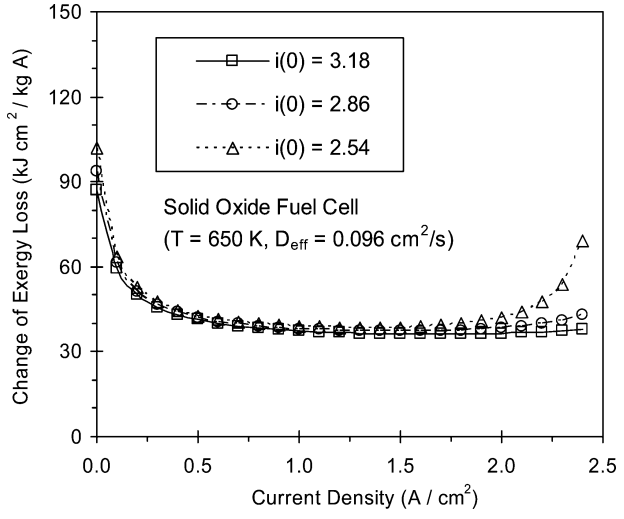

Fig. 7 Change of exergy destruction at varying current densities.

current density. In Fig. 6, concentration irreversibilities occur from a change of reactant concentration at the electrode surface during the chemical reaction. Failure to transport sufficient reactant to the electrode hinders the chemical reaction and causes irreversible losses of exergy. In Fig. 6, this irreversibility rises at larger current densities, due to larger concentration changes needed to sustain more chemical activity at the electrode surfaces.

Adverse impact from changes of fuel cell design parameters can be minimized by considering when changes of entropy production are minimal. Figure 7 illustrates that the derivative of exergy loss is minimum at current densities of about 1.5 A/cm^2. Thus, changes in operating conditions near this point will not appreciably affect the overall efficiency. However, changes below 0.5 A/cm^2 or above 2.0 A/cm^2 will more drastically raise exergy losses. In Fig. 7, the exergy loss increases more rapidly at lower exchange current densities, as the chemical activity at the electrode surface changes more rapidly to drive larger electric currents.

Comparing Figs. 4 and 8, it can be observed that the unit irreversibility ratio increases less rapidly at low current densities for an SO fuel cell, as compared with a PEM fuel cell. In the former case, activation irreversibilities rise less rapidly at low current densities. Also, concentration losses increase nearly linearly and exceed activation irreversibilities, so the relative contributions to the total exergy loss are notably different in SO fuel cells. In an SO fuel cell, the conductivity of materials typically decreases at lower temperatures, thereby increasing ohmic losses within the fuel cell. Figure 8 illustrates that the unit irreversibility ratio increases at lower temperatures. Thus, the performance of an SO fuel cell decreases when

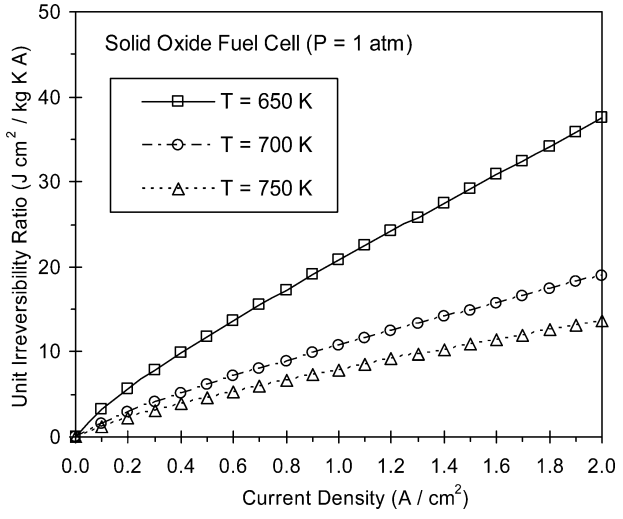

Fig. 8 Entropy production per unit current flow.

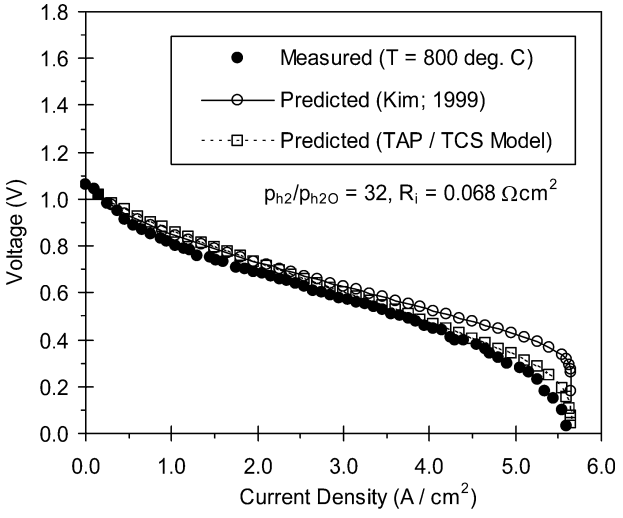

Fig. 9 Comparison of predicted SOFC voltage with measured data ($T = 800°$C).

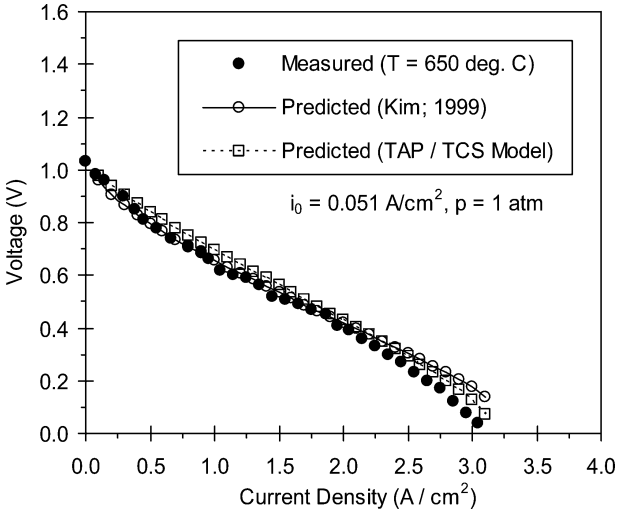

Fig. 10 Comparison of predicted SOFC voltage with measured data ($T = 650°$C).

the operating temperature is lowered. Unfortunately, lower temperatures are advantageous due to lower costs of materials and construction. As a result, a major focus of SO fuel cell research is developing electrodes and electrolytes that operate better at low temperatures.

In Figs. 9 and 10, close agreement between the predicted voltage profile and measured data[19] can be observed. Better accuracy is obtained with the current TAP/TCS model, especially at the higher temperature ($T = 800°C$) and high current densities. Unlike past predictions by Kim and co-workers,[19] voltage predictions in the TAP/TCS model were calculated based on the entropy production of combined ohmic, concentration and activation irreversibilities. In Figs. 9 and 10, it can be observed that the voltage falls more rapidly at the lower temperature. It is advantageous to operate at lower temperatures in certain applications, such as developments by BMW to use SO fuel cells as an auxiliary power supply in vehicles. However, high operating temperatures are needed in other applications. For example, high-temperature fuel cells are needed in a bottoming cycle of an SOFC combined cycle or hybrid system for power generation.

This article has developed and modeled exergy losses due to activation energy and cathode polarization within the membrane electrode assembly, while a companion article has considered additionally the friction and thermal irreversibilities of gas flow through the fuel channels.[21] Entropy production due to heat transfer and gas friction requires additional modeling of the coupled mass and momentum equations within the fuel channel. When fuel channel and membrane electrode assembly irreversibilities are combined, the entropy-based design provides a unified formulation for characterizing all sources of effective voltage losses within a fuel cell.

VII. Conclusions

In this article, entropy production of thermochemical irreversibilities in a fuel cell has been related to cell voltage losses (or cell polarization). A predictive formulation of activation polarization was developed with the Butler–Volmer equation. A one-dimensional diffusion approximation was used to predict the concentration polarization within a cathode. Unlike past studies of entropy production in a solid oxide fuel cell, this article formulates half-cell reaction kinetics for exergy losses in a proton-exchange membrane fuel cell. In contrast to SO fuel cells, the predicted results have shown that activation exergy losses in a PEM fuel cell exceed ohmic losses. The unit irreversibility ratio increases rapidly at low current densities, due to the rapid change of activation overpotential. The concentration irreversibility rises at high current densities, because larger concentration changes are needed to sustain more chemical activity at the electrode surfaces. Failure to transfer sufficient reactant to the electrode hinders the chemical reaction and causes entropy production. In conclusion, entropy production is believed to provide a useful parameter for characterizing fuel cell performance. An entropy-based design encompasses all types of irreversibilities, but allows a systematic procedure for improving fuel cell performance over a range of operating conditions.

Acknowledgment

Support of this research from the Natural Sciences and Engineering Research Council of Canada is gratefully acknowledged.

References

[1]Burke, K. A., "Fuel Cells for Space Science Applications," AIAA Paper 2003-5938, Aug. 2003.

[2]Barbir, F., Dalton, L., and Molter, T.,"Regenerative Fuel Cells for Energy Storage: Efficiency and Weight Trade-Offs," AIAA Paper 2003-5937, Aug. 2003.

[3]Chang, B., Johnson, D., Garcia, C., Jakupca, I., Scullin, V., and Bents, D., "Regenerative Fuel Cell Test Rig at Glenn Research Center," AIAA Paper 2003-5942, Aug. 2003.

[4]Sridhar, K. R., and Foerstner, R., "Regenerative CO/O_2 Solid Oxide Fuel Cells for Mars Exploration," AIAA Paper 98-650, Jan. 1998.

[5]Hottinen, T., Himanen, O., and Lund, P., "Performance of Planar Free-Breathing PEMFC at Temperatures Below Freezing," *Journal of Power Sources* (to be published).

[6]Xu, R., and Naterer, G. F., "Controlling Phase Interface Motion in Inverse Heat Transfer Problems with Solidification," *Journal of Thermophysics and Heat Transfer*, Vol. 17, No. 4, 2003, pp. 488–497.

[7]Sundaresan, M., and Moore, R., "Polymer Electrolyte Fuel Cell Stack Thermal Model to Evaluate Sub-freezing Startup," *Journal of Power Sources*, Vol. 145, No. 2, 2005, pp. 534–545.

[8]Naterer, G. F., *Heat Transfer in Single and Multiphase Systems*, CRC Press, Boca Raton, FL, 2002.

[9]Naterer, G. F., "Applying Heat–Entropy Analogies with Experimental Study of Interface Tracking in Phase Change Heat Transfer," *International Journal of Heat and Mass Transfer*, Vol. 44, No. 15, 2001, pp. 2917–2932.

[10]Kimble, M., and Hoberecht, M., "Performance Evaluation of ElectroChem's PEM Fuel Cell Power Plant for NASA's 2nd Generation Reusable Launch Vehicle," AIAA Paper 2003-5966, Aug. 2003.

[11]Mawardi, A., Yang, F., and Pitchumani, R., "Optimization of the Operating Parameters of a Proton Exchange Membrane Fuel Cell for Maximum Power Density," *ASME Journal of Fuel Cell Science and Technology*, Vol. 2, No. 2, 2005, pp. 121–135.

[12]Wang, D., Naterer, G. F., and Wang, G., "Thermofluid Optimization of a Heated Helicopter Engine Cooling Bay," *Canadian Aeronautics and Space Journal*, Vol. 49, No. 2, 2003, pp. 73–86.

[13]Naterer, G. F., "Adaptive Surface Micro-Profiling for Microfluidic Energy Conversion," *Journal of Thermophysics and Heat Transfer*, Vol. 18, No. 4, 2004, pp. 494–501.

[14]Chan, S. H., and Xia, Z. T., "Polarization Effects in Electrolyte/Electrode-Supported Solid Oxide Fuel Cells," *Journal of Applied Electrochemistry*, Vol. 32, 2002, pp. 339–347.

[15]Song, S., Douvartzides, S., and Tsiakaras, P., "Exergy Analysis of an Ethanol Fuelled Proton Exchange Membrane (PEM) Fuel Cell System for Automobile Applications," *Journal of Power Sources* (to be published).

[16]Ghadamian, H., and Saboohi, Y., "Quantitative Analysis of Irreversibilities Causes Voltage Drop in Fuel Cell (Simulation and Modeling)," *Electrochimica Acta*, Vol. 50, 2004, pp. 699–704.

[17]Hussain, M. M., Baschuk, J. J., Li, X., and Dincer, I., "Thermodynamic Analysis of a PEM Fuel Cell Power System," *International Journal of Thermal Sciences*, Vol. 44, 2005, pp. 903–911.

[18]Bossel, U., "Efficiency of Hydrogen Fuel Cell, Diesel-SOFC-Hybrid and Battery Electric Vehicles," European Fuel Cell Forum, Morgenacherstrasse, Germany, Oct. 20, 2003.

[19]Kim, J. W., Virkar, A. V., Fung, K. Z., Mehta, K., and Singhal, S. C., "Low Temperature, High Performance Anode-Supported Solid Oxide Fuel Cells," *Journal of the Electrochemical Society*, Vol. 146, 1999, pp. 69–78.

[20]Chen, F., Wen, Y. Z., Chu, H. S., Yan, W. M., and Soong, C. Y., "Convenient Two-Dimensional Model for Design of Fuel Channels for Proton Exchange Membrane Fuel Cells," *Journal of Power Sources*, Vol. 128, 2004, pp. 125–134.

[21]Naterer, G. F., and Tokarz, C. D., "Entropy Based Design of Fuel Cells," *ASME Journal of Fuel Cell Science and Technology* (to be published).